Evaluating Uncertainties in the Projection of Future Drought

ELEANOR J. BURKE AND SIMON J. BROWN

Hadley Centre, Met Office, Exeter, United Kingdom

(Manuscript received 7 May 2007, in final form 15 August 2007)

ABSTRACT

The uncertainty in the projection of future drought occurrence was explored for four different drought indices using two model ensembles. The first ensemble expresses uncertainty in the parameter space of the third Hadley Centre climate model, and the second is a multimodel ensemble that additionally expresses structural uncertainty in the climate modeling process. The standardized precipitation index (SPI), the precipitation and potential evaporation anomaly (PPEA), the Palmer drought severity index (PDSI), and the soil moisture anomaly (SMA) were derived for both a single CO_2 ($1\times CO_2$) and a double CO_2 ($2\times CO_2$) climate. The change in moderate drought, defined by the 20th percentile of the relevant $1\times CO_2$ distribution, was calculated. SPI, based solely on precipitation, shows little change in the proportion of the land surface in drought. All the other indices, which include a measure of the atmospheric demand for moisture, show a significant increase with an additional 5%–45% of the land surface in drought. There are large uncertainties in regional changes in drought. Regions where the precipitation decreases show a reproducible increase in drought across ensemble members and indices. In other regions the sign and magnitude of the change in drought is dependent on index definition and ensemble member, suggesting that the selection of appropriate drought indices is important for impact studies.

1. Introduction

Drought can have a significant impact on the socioeconomic state of the population. Therefore, drought events are carefully monitored in order to help mitigate associated losses and to manage impacts. In addition, it is important to investigate how drought might change under future climate change scenarios using relevant drought metrics. Results from these studies can be used to inform impacts and develop adaptation strategies.

Definitions of drought depend on the nature of the water deficit and the objective of its use (American Meteorological Society 1997). There are three main types of drought: 1) meteorological drought, which is usually defined as a drying relative to the mean state; 2) agricultural drought, which results in a reduced supply of moisture for crops; and 3) hydrological drought associated with a deficit in the supply of surface and subsurface water. Hence, there are a whole range of different drought indices (Keyantash and Dracup 2002) that are more or less relevant to each drought classification and that are usually dependent on some combination of precipitation, temperature, potential evaporation, runoff, and soil moisture. Future projections of drought will depend on the specific definition of drought used.

General circulation models (GCMs) have been used previously to investigate water availability. For example, Wetherald and Manabe (2002) and Manabe et al. (2004) showed a global increase in runoff rate under future climate scenarios, possibly suggesting less hydrological drought. Summer drying in many parts of the northern subtropics and midlatitudes is a key feature of the majority of models (Rowell and Jones 2006; Seneviratne et al. 2002; Meehl et al. 2006) although with a large variation in amplitude between models (Wang 2005), possibly suggesting an increase in meteorological and agricultural drought over these regions. Burke et al. (2006) used the third climate configuration of the Met Office Unified Model (HadCM3) and projected that, if greenhouse gas emissions follow the A2 scenario (Solomon et al. 2007), an additional 30% of the land surface would be in drought by the end of the century. They defined drought using the Palmer drought severity index (PDSI), a widely accepted meteorological drought index.

Corresponding author address: Eleanor J. Burke, Hadley Centre, Met Office, Fitzroy Road, Exeter EX1 3PB, United Kingdom. E-mail: eleanor.burke@metoffice.gov.uk

DOI: 10.1175/2007JHM929.1

This work addresses the sensitivity of projections of future drought to index definition and model uncertainties. Four different drought indices were calculated at time scales of 12 months using output from two ensembles of climate model simulations: a large 128-member perturbed physics ensemble and an 11-member multimodel ensemble. Simulations made under double CO_2 ($2\times CO_2$; 560 ppm) conditions were compared with preindustrial CO_2 ($1\times CO_2$; 280 ppm) runs. Uncertainties in global changes in drought were assessed along with the reproducibility of regional changes.

2. Model ensembles

a. Hadley Centre climate model multiparameter ensemble

The multiparameter ensemble (MPE) is described by Webb et al. (2006). It consists of 128 versions of version three of the Hadley Centre Atmospheric Climate Model (HadAM3; Pope et al. 2000) coupled to a 50-m nondynamic mixed layer ("slab") ocean. HadAM3 incorporates the Met Office Surface Exchange Scheme (MOSES) land surface scheme, which has a four-layer soil model (Cox et al. 1999). Multiple model parameters were simultaneously perturbed for each ensemble member. These parameters directly influence the following processes: large-scale cloud, convection, radiation, boundary layer, dynamics, land surface, and sea ice and are detailed by Collins et al. (2006). The parameter that has most relevance here is whether the plants stomata respond to increased CO_2 or not; if they respond there is a decrease in evapotranspiration and increase in temperature with increasing CO_2 (Betts et al. 2007). The perturbations were selected to result in a range of climate sensitivities (the difference in global mean temperature between $1\times CO_2$ and $2\times CO_2$ simulations) and maximize coverage of parameter space and model skill (Webb et al. 2006; Collins et al. 2006). Each of the model simulations have a stable climate and are in equilibrium with the atmospheric CO_2 concentration. The effect of increasing CO_2 was studied for each ensemble member by comparing simulations with preindustrial ($1\times CO_2$) and double CO_2 ($2\times CO_2$) concentrations.

b. Multimodel ensemble

MPE only includes uncertainty in parameter selection for one climate model. The much smaller multimodel ensemble (MME) includes a range of structural perturbations that encompass a variety of physical parameterizations and spatial resolutions. It might be expected that MME will have greater variability than MPE. However, the parameters in MPE were selected specifically to generate a wide range of climate sensitivities (2.3°–6.0°C). This range is slightly larger than that within the multimodel ensemble (2.1°–4.3°C).

Eleven of the models participating in the Intergovernmental Panel on Climate Change (IPCC) Fourth Assessment were used here (Solomon et al. 2007): the Canadian Centre for Climate Modelling and Analysis (CCCma) Coupled General Circulation Model, version 3.1 (CGCM3.1; T47 and T63); Commonwealth Scientific and Industrial Research Organisation Mark version 3.0 (CSIRO Mk3.0); Goddard Institute for Space Studies Model E-R (GISS-ER); Institute of Numerical Mathematics Coupled Model, version 3.0 (INM-CM3.0); Model for Interdisciplinary Research on Climate 3.2 [MIROC3.0; medium- and high-resolution versions (medres and hires)]; ECHAM5/Max Planck Institute Ocean Model (MPI-OM); Meteorological Research Institute Coupled General Circulation Model, version 2.3.2 (MRI CGCM2.3.2); Community Climate System Model, version 3 (CCSM3); and Met Office Hadley Centre Global Environmental Model, version 1 (UKMO-HadGEM1). These models were selected because of the availability of at least 20 yr of slab equilibrium experiments at $1\times CO_2$ and $2\times CO_2$, which correspond to MPE. It should be noted that each model in MME has its own land surface scheme with its own definition of total soil profile depths and layer thicknesses.

3. Drought indices

a. Standardized precipitation index (SPI)

The SPI is a meteorological drought index that provides a comparison of the precipitation over the preceding 12-month period with the corresponding climatology. It is estimated by transforming the long-term precipitation distribution for each location to a normal distribution (Guttman 1999). The location-specific parameters used to transform the $1\times CO_2$ precipitation distribution were also used to transform the $2\times CO_2$ precipitation distribution. Because the SPI is based solely on precipitation it is readily available and useful for planners and policy makers.

b. Precipitation potential evaporation anomaly (PPEA)

The PPEA provides an alternate estimate of meteorological drought at time scales of 12 months. It is given by

$$\mathrm{PPEA} = (P - P_c) - (\mathrm{PE} - \mathrm{PE}_c), \qquad (1)$$

where P and PE are the average values of the precipitation and potential evaporation for the preceding 12

TABLE 1. The mean change in the percentage of the global land surface in drought with the 5th–95th percentile range shown in brackets. Figure 1 shows the distribution of the change in ΔD^{20} for the different indices.

	MPE: mean (5th–95th percentile)			MME: mean (5th–95th percentile)		
	ΔD^1	ΔD^5	ΔD^{20}	ΔD^1	ΔD^5	ΔD^{20}
ΔD_{SPI}	5 (3, 9)	5 (2, 10)	2 (−1, 9)	3 (2, 5)	3 (0, 5)	0 (−3, 3)
ΔD_{PPEA}	24 (15, 35)	30 (21, 41)	33 (25, 43)	21 (17, 31)	26 (22, 36)	27 (24, 37)
ΔD_{PDSI}	23 (16, 33)	26 (19, 36)	26 (19, 36)	19 (12, 25)	21 (13, 27)	20 (11, 26)
ΔD_{SMA}	14 (9, 18)	15 (10, 21)	12 (7, 19)	17 (7, 24)	18 (8, 26)	13 (6, 27)

months, and P_c and PE_c are the 20-yr precipitation and potential evaporation climatologies, respectively. The climatologies for $1\times CO_2$ conditions were also used to calculate the PPEA under $2\times CO_2$ conditions.

c. Palmer drought severity index

The PDSI was created by Palmer (1965) to provide the "cumulative departure of moisture supply" from the normal. Full details of the PDSI calculation can be found at the National Agricultural Decision Support System Web site (http://nadss.unl.edu). As suggested by Burke et al. (2006), the potential evaporation required as input to the PDSI was calculated using the Penman–Monteith equation (Shuttleworth 1993) instead of the Thornthwaite (1948) equation. Analysis shows that the PDSI has a memory of the order of 12 months, resulting in the use of this time scale for the other indices. Despite being developed to provide an estimate of meteorological drought, published comparisons between the PDSI and soil moisture (e.g., Sheffield et al. 2004) suggest that the PDSI might also give some indication of agricultural drought. Calibration parameters determined for each location under $1\times CO_2$ conditions were held constant when calculating the PDSI for $2\times CO_2$ conditions.

d. Soil moisture anomaly

The soil moisture anomaly (SMA) is a highly relevant index for vegetative health and agricultural production and is calculated within the climate models. However, limited observations of soil moisture mean that operationally this is not often a practical drought index. The SMA, at time scales of 12 months, was calculated for the whole soil moisture profile by subtracting the soil moisture climatology [cf. Eq. (1)]. The same climatology was used for $1\times CO_2$ and $2\times CO_2$ conditions.

4. Definition of drought

Time series of the drought indices were calculated over the majority of land grid cells for the two model ensembles. Cold regions, defined as grid cells where the temperature is less than 0°C for greater than six months of the year and spends less than three months of the year greater than 6°C (Deichmann and Eklundh 1991, 29–32) were excluded, mainly because the PDSI does not include frozen processes so will likely have a high error in these regions. Temperatures were based on the mean climatology for $1\times CO_2$ MPE.

Threshold values for drought were defined using the distributions of the drought indices for the $1\times CO_2$ simulations. For each grid cell and ensemble member the values of the 1st, 5th, and 20th percentile of the distribution were taken to be the threshold for extreme, severe, and moderate drought, respectively. Therefore, by definition, for $1\times CO_2$ the average proportion of the land surface in extreme, severe, and moderate drought is 1%, 5%, and 20%, respectively. The fraction of the land surface in drought for $2\times CO_2$ is given by the proportion of the grid cells where the drought index is less than the relevant threshold. Each distribution contains a limited set of data: only 240 months. Analysis of the same indices using a larger sample size (3600 months) shows a small low bias of 0.02 in the change in the proportion of the land surface in drought. This is consistent across ensemble members and indices and therefore does not contribute to uncertainties.

5. Results

a. Uncertainty in global drought projections

The ensemble mean of global land surface change in extreme (1st percentile), severe (5th percentile), and moderate (20th percentile) drought (ΔD^1, ΔD^5, and ΔD^{20}, respectively) as a result of doubling atmospheric CO_2, together with their uncertainties are presented in Table 1 for SPI, PPEA, PDSI, and SMA (ΔD_{SPI}, ΔD_{PPEA}, ΔD_{PDSI}, and ΔD_{SMA}, respectively). For all but MME $\Delta D^{20}_{\mathrm{SPI}}$ the ensemble mean change shows an increase drought, which is generally significantly different from zero at the 5%–95% level. MME mean values are often slightly lower than those for MPE but agree within the 5%–95% range. MPE has larger uncertainty ranges than MME for all indices except SMA; this

TABLE 2. The correlation coefficients between the different drought indices for the two ensembles.

	PPEA	PDSI	SMA
SPI	0.66	0.78	0.46
PPEA		0.85	0.09
PDSI			0.21

could be because the models in MME are more likely to reflect global observations of precipitation and temperature than the models in MPE. Global distributions of soil moisture are not available for model evaluation, and large structural differences between the land surface schemes results in larger uncertainties in MME SMA (Pitman et al. 1999) compared with the uncertainties in MPE.

Both the spread and ensemble mean values of ΔD are relatively independent of drought threshold. This has serious implications for the more serious droughts. For example, Table 1 shows an increase of approximately 20% of the global land surface in both $\Delta D^{20}_{\mathrm{PDSI}}$ and $\Delta D^{1}_{\mathrm{PDSI}}$. This means that the area under moderate drought increases from 20% to 40% of the land surface, whereas the area under extreme drought increases much more dramatically, from 1% to 21% of the land surface.

The change in drought is highly dependent on the index definition, with ΔD_{SPI} showing the smallest changes and ΔD_{PPEA} the largest. SPI is derived solely from precipitation whereas PPEA also includes atmospheric demand for moisture, which increases with increasing temperature. The PDSI and SMA include atmospheric demand for moisture but this demand is moderated by land surface processes. For PDSI this was calculated using a simple bucket model, while the climate models include a more complete representation of the land surface. Overall, increases in drought are generally smaller for ΔD_{SMA} than for ΔD_{PDSI}. Table 2 shows the correlations between different indices calculated using ΔD for each MPE ensemble member: ΔD_{SPI} is generally well correlated with all other indices, although rather weakly for $\Delta \mathrm{D}_{\mathrm{SMA}}$; $\Delta \mathrm{D}_{\mathrm{PPEA}}$ is well correlated with ΔD_{PDSI} and both are poorly correlated with ΔD_{SMA}. A major contribution to this poor correlation between ΔD_{PDSI} and ΔD_{SMA} is the relative impact of the stomata response to increased CO_2 on the different drought indices. Figure 1 shows the probability distribution of ΔD^{20} for the two ensembles. The MPE ensemble is split into two subensembles (stomata response to increased CO_2 is either on or off). This parameter significantly increases uncertainties in ΔD_{PDSI}, slightly increases uncertainties in ΔD_{SPI} and ΔD_{PPEA}, but has little impact on uncertainties ΔD_{SMA}. Understanding the reasons for these differences is the subject of further work.

The dominance of atmospheric demand on global mean changes of PPEA (and similarly although to a lesser degree for PDSI and SMA) is illustrated in Fig. 2. Figure 2a shows ΔD for each MPE member calculated using potential evaporation from $1\times CO_2$ conditions and precipitation representative of $2\times CO_2$. In Fig. 2b, ΔD is calculated using precipitation from $1\times CO_2$ conditions and potential evaporation from $2\times CO_2$. Representative $2\times CO_2$ precipitation/potential evaporation was obtained by adding changes from $1\times CO_2$ to $2\times CO_2$ to the $1\times CO_2$ climatologies. Changes in precipitation alone have little impact on the ensemble mean ΔD with a suggestion of a decrease in drought. However, changes in potential evaporation alone produce substantial increases in drought.

b. Uncertainty in regional drought projections

Although the majority of ensemble members and indices show an increase in global mean ΔD, regionally this is not the case (Fig. 3). SPI, the index based solely on precipitation (Figs. 3a,b), shows a consistent increase in moderate drought for both ensembles over the Mediterranean and southern Africa, with an indication of common drying in Amazonia, Central America, and Australia. The occurrence of SPI-based drought consistently decreases in North America, central Eurasia, and parts of South America and Africa. This pattern of change is well correlated with annual mean precipitation changes between $1\times CO_2$ and $2\times CO_2$ climates and explains the small global mean SPI changes in Table 1. The level of agreement between MPE and MME is encouraging given the diverse nature of the two ensembles.

PPEA, the index that includes both precipitation and unmitigated atmospheric demand for moisture, shows a consistent increase in drought over the majority of the land surface (Figs. 3c,d). Exceptions to this include Indo-China and small regions in central Africa and South America. MME has more regions with uncertain changes such as Canada and a region of reduced drought east of Finland, both consistent with regions of stronger wetting seen in the MME SPI.

The simple surface representation of PDSI moderates the increase in drought seen with PPEA with smaller areas showing consistent drying (Figs. 3e,f) and larger areas showing no change or a decrease. However, the general pattern of change remains the same.

Soil moisture reflects both changes in precipitation and the interaction between land surface processes, plants, and atmospheric demand. Overall the increase in drought is slightly lower than for the PDSI. In MPE,

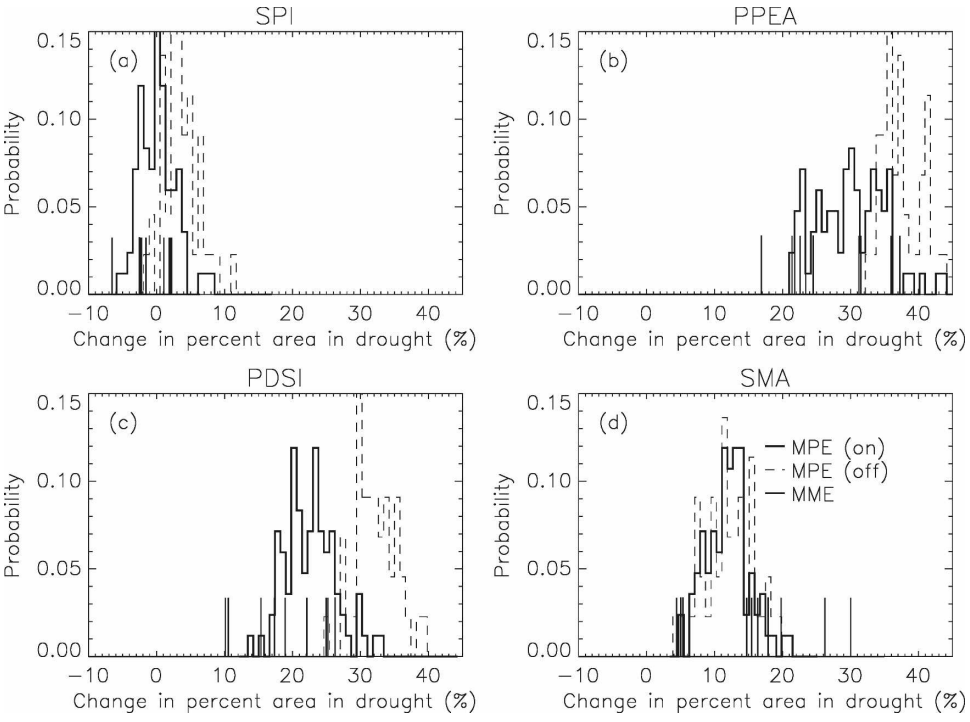

FIG. 1. Frequency distribution of the change in the percentage of the land surface in moderate drought for the two model ensembles and four different drought indices: (a) $\Delta D^{20}_{\mathrm{SPI}}$, (b) $\Delta D^{20}_{\mathrm{PPEA}}$, (c) $\Delta D^{20}_{\mathrm{PDSI}}$, and (d) $\Delta D^{20}_{\mathrm{SMA}}$. The dashed line represents the probability distribution of the MPE ensemble with the stomata responding to increased CO_2, the gray line represents the probability distribution of the MPE ensemble when the stomata do not respond to increased CO_2, and the black lines each represent one member of the MME ensemble.

the likely change in SMA-based drought (Fig. 3g) south of ~45°N reflects changes in precipitation (represented by Fig. 3a). There is a consistent increase in drought at higher latitudes because a greater proportion of the soil water is unfrozen in $2\times CO_2$ and available for increased evapotranspiration. In MME, the likely change in drought (Fig. 3h) correlates well with precipitation changes at all latitudes. Although only moderate drought is discussed here, these results are representative of drought of other severities.

Figure 4 summarizes the uncertainty in the change in drought for specific regions: Australia, South America, North America, Indo-China, South Africa, and the Mediterranean. As for the case of global drought, the regional average change in the proportion of land surface in drought (Δd) was calculated for each ensemble

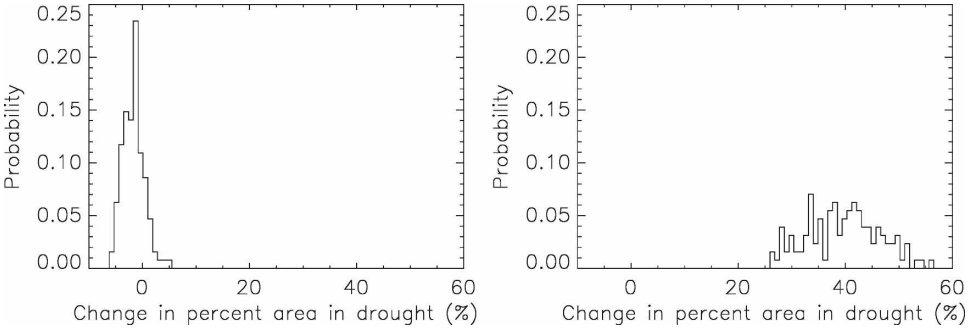

FIG. 2. The frequency distribution of the change in the proportion of the land surface in moderate drought for a modified version of the PPEA: (a) precipitation representative of $2\times CO_2$ and potential evaporation from $1\times CO_2$ and (b) precipitation from $1\times CO_2$ and potential evaporation representative of $2\times CO_2$.

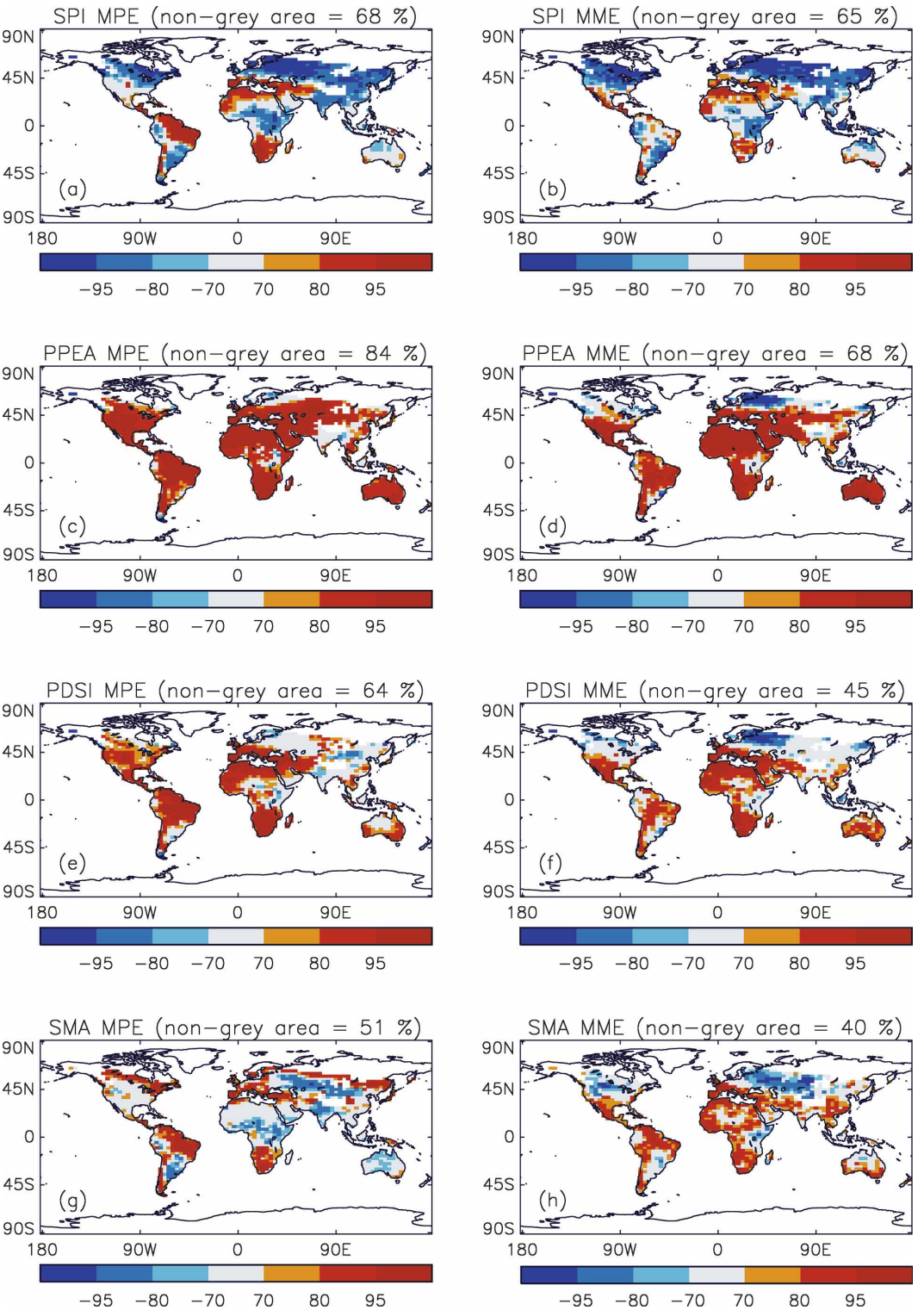

FIG. 3. Spatial distribution of the likelihood of increase or decrease of moderate drought for MPE and MME. Locations where more than 70% of the ensemble members show a decrease (increase) in moderate drought are in blue (red). Places where less than 70% of the ensemble members agree on either an increase or a decrease are in gray. The percentage of the total area where more than 70% of the models agree is given.

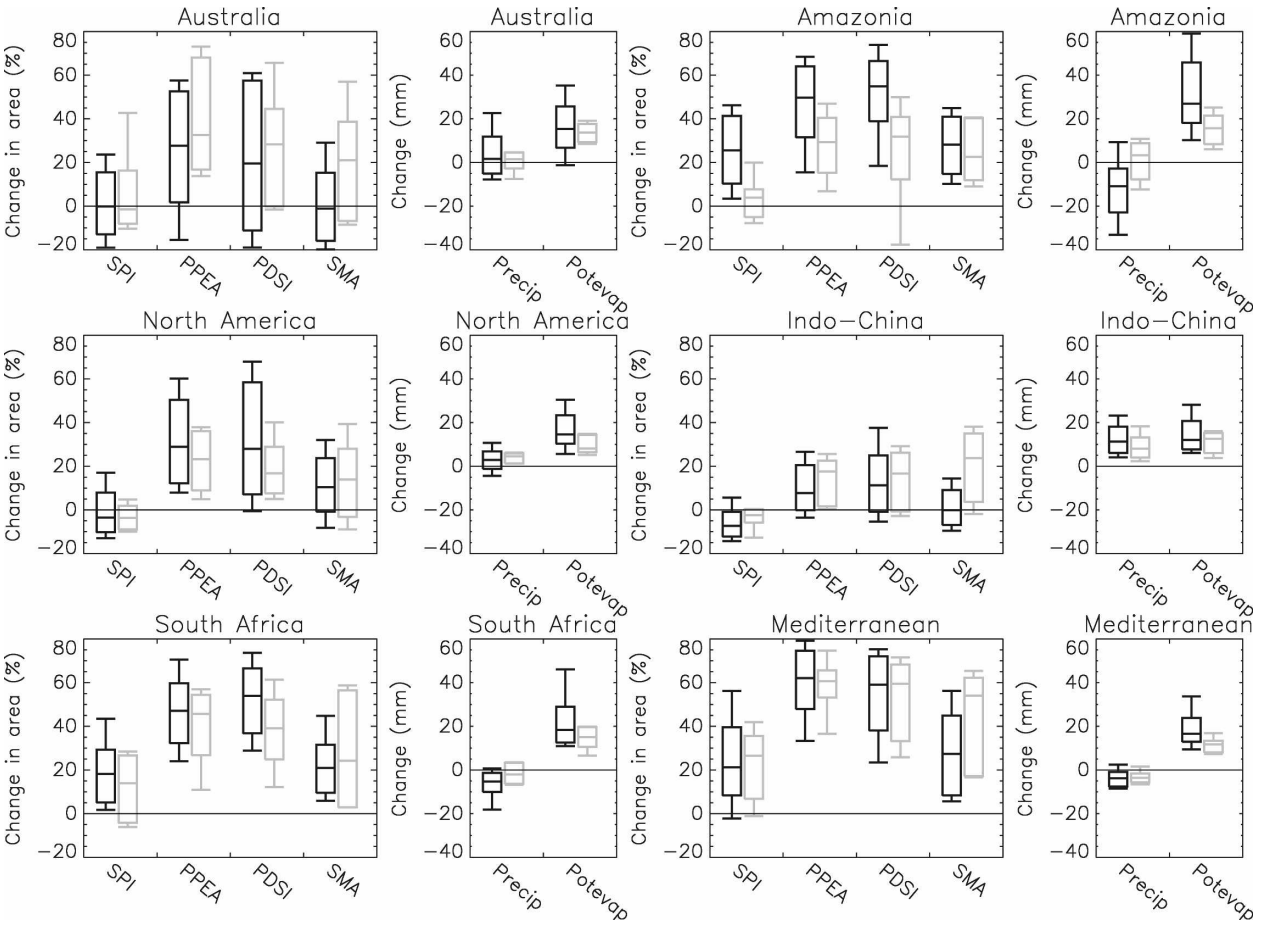

FIG. 4. The uncertainty in the change in the percentage of the land surface in drought for selected regions along with the uncertainty in changes in precipitation and potential evaporation. MPE is shown in black and MME in gray. The box shows the 25th to 75th uncertainty range and the whiskers show the 5th to 95th uncertainty range.

member. Also shown is the uncertainty in changes in potential evaporation and precipitation for each region.

For all regions there is a large uncertainty in the change in drought, which is dependent on region, index, and ensemble. Both ensembles have virtually all members producing increased potential evaporation with ensemble medians ranging from 8 to 26 mm month^{-1}. However, for precipitation the sign and magnitude of changes and their uncertainty are more dependent on region, so it appears that for regional changes in drought precipitation is the dominant driver, both in the sign of change and the degree of uncertainty.

The Mediterranean, Amazonia, and South Africa predominantly have a reduction in precipitation, which with the increase in potential evaporation results, for the most part, in substantial increases in drought. Australia has the largest uncertainty in changes in drought, with the distribution of precipitation changes for Australia centered on zero. North America shows a similar (but moderated) response to Australia. In Indo-China, the small increase in precipitation is comparable to the increase in potential evaporation resulting in smaller uncertainties.

6. Discussion and conclusions

Changes in drought between a preindustrial climate (280 ppm atmospheric CO_2) and a double CO_2 climate were calculated for four different drought indices from two different ensembles. The first ensemble expresses uncertainty in the parameter space of the third Hadley Centre climate model, and the second expresses structural uncertainty in the climate modeling process using multiple models.

Atmospheric demand for moisture increases universally, consistent with higher atmospheric temperatures due to the CO_2 increase. Therefore, atmospheric demand needs to be included if realistic impacts are to be assessed. The soil moisture from the climate models should include the best estimate of atmospheric demand. However, drought projections using model-

calculated soil moisture should be treated with caution because of the lack of suitable observations for verification.

All indices that include some measure of the atmospheric demand for moisture (PPEA, PDSI, and SMA) show increases in the proportion of the global land surface in drought ranging from an additional 5%–45%. SPI, based solely on precipitation, shows much smaller global changes ranging from 5% less to 10% more of the land surface. In addition to the overall increase in area affected by drought, the area in more severe drought increases much more than the area in less severe drought. This could have serious consequences as the impact of drought on socioeconomics increases with the severity of drought.

Regionally, there is a very large range in the sign and magnitude of drought changes. The only regions where there is a consistent increase in drought across all indices and ensembles are those where the annual average precipitation decreases as found for the Mediterranean, Amazonia, and southern Africa. In other regions the sign and magnitude of the change in drought is dependent on index definition and ensemble member.

The impact of change in drought will be felt at the regional scale. Therefore, in order to perform optimum impact assessments of changes in drought, regional studies are required using locally appropriate drought indices. For example, a soil-moisture-based drought index on a daily basis over the growing season will be most relevant for studying the impacts in agriculture. Furthermore, local practices not included in the climate model will need to be taken into account, for example, irrigation, where remote changes may be significant. However, the fullest expression of modeling uncertainty is desirable if robust adaptation plans are to be formed.

Acknowledgments. This work was funded by the Department for Environment, Food, and Rural Affairs under Contract PECD 7/12/37. We acknowledge the QUMP team at the Met Office Hadley Centre who created the multiparameter ensemble. The multimodel data were provided by the different modeling groups via the Program for Climate Model Diagnosis and Intercomparison (PCMDI), which is supported by the Office of Science, U.S. Department of Energy.

REFERENCES

American Meteorological Society, 1997: Meteorological drought—Policy statement. *Bull. Amer. Meteor. Soc.,* **78,** 847–849.

Betts, R. A., and Coauthors, 2007: Plant responses double the impact of CO2-induced climate change on simulated future runoff. *Nature,* **448,** 1037–1041.

Burke, E. J., S. J. Brown, and N. Christidis, 2006: Modeling the recent evolution of global drought and projections for the 21st century with the Hadley Centre climate model. *J. Hydrometeor.,* **7,** 1113–1125.

Collins, M., B. B. B. Booth, G. Harris, J. M. Murphy, D. M. H. Sexton, and M. Webb, 2006: Towards quantifying uncertainty in transient climate change. *Climate Dyn.,* **27,** 127–147.

Cox, P. M., R. A. Betts, C. B. Bunton, R. H. Essery, P. R. Rowntree, and J. Smith, 1999: The impact of new land surface physics on the GCM simulation of climate and climate sensitivity. *Climate Dyn.,* **15,** 183–203.

Deichmann, U., and L. Eklundh, 1991: Global digital data sets for land degradation studies: A GIS approach. GRID Case Study Series 4, UNEP/GEMS and GRID, Nairobi, Kenya, 103 pp.

Guttman, N. B., 1999: Accepting the Standardized Precipitation Index: A calculation algorithm. *J. Amer. Water Resour. Assoc.,* **35,** 311–322.

Keyantash, J., and J. A. Dracup, 2002: The quantification of drought: An evaluation of drought indices. *Bull. Amer. Meteor. Soc.,* **83,** 1167–1180.

Manabe, S., R. T. Wetherald, P. C. D. Milly, T. L. Delworth, and R. J. Stouffer, 2004: Century-scale change in water availability: CO2-quadrupling experiment. *Climatic Change,* **64,** 59–76.

Meehl, G. A., and Coauthors, 2006: Climate change projections for the twenty-first century and climate change commitment in the CCSM3. *J. Climate,* **19,** 2597–2616.

Palmer, W. C., 1965: Meteorological drought. U.S. Weather Bureau Research Paper 45, 85 pp. [Available from NOAA/Library and Information Services Division, Washington, DC 20852.]

Pitman, A. J., and Coauthors, 1999: Key results and implications from phase 1(c) of the Project for Intercomparison of Land-Surface Parameterization Schemes. *Climate Dyn.,* **15,** 673–684.

Pope, V. D., M. Gallani, P. R. Rowntree, and R. A. Stratton, 2000: The impact of new physical parameterisations in the Hadley Centre climate model—HadAM3. *Climate Dyn.,* **16,** 123–146.

Rowell, D. P., and R. G. Jones, 2006: Causes and uncertainty of future summer drying over Europe. *Climate Dyn.,* **27,** 281–299.

Seneviratne, S. I., J. S. Pal, E. A. B. Eltahir, and C. Schar, 2002: Summer dryness in a warmer climate: A process study with a regional climate model. *Climate Dyn.,* **20,** 69–85.

Sheffield, J., G. Goteti, F. Wen, and E. F. Wood, 2004: A simulated soil moisture based drought analysis for the United States. *J. Geophys. Res.,* **109,** D24108, doi:10.1029/2004JD005182.

Shuttleworth, W. J., 1993: Evaporation. *Handbook of Hydrology,* D. R. Maidment, Eds., McGraw-Hill, 4.1–4.53.

Solomon, S., D. Qin, M. Manning, M. Marquis, K. Averyt, M. M. B. Tignor, H. L. Miller Jr., and Z. Chen, Eds., 2007: *Climate Change 2007: The Physical Sciences Basis.* Cambridge University Press, 996 pp.

Thornthwaite, C. W., 1948: An approach toward a rational classification of climate. *Geogr. Rev.,* **38,** 55–94.

Wang, G. L., 2005: Agricultural drought in a future climate: Results from 15 global climate models participating in the IPCC 4th assessment. *Climate Dyn.,* **25,** 739–753.

Webb, M. J., and Coauthors, 2006: On the contribution of local feedback mechanisms to the range of climate sensitivity in two GCM ensembles. *Climate Dyn.,* **27,** 17–38.

Wetherald, R. T., and S. Manabe, 2002: Simulation of hydrologic changes associated with global warming. *J. Geophys. Res.,* **107,** 4379, doi:10.1029/2001JD001195.